

# SIMULATION OF PANCAKE ICE IN A WAVE FIELD

Mark A. Hopkins<sup>1</sup>, Member ASCE and Hayley H. Shen<sup>2</sup>, Member ASCE

## INTRODUCTION

From many field observations, it has become well known that pancake ice is ubiquitous in a wave dominated sea. These strikingly uniform circular floes are consistently found in Antarctic seas during the ice formation season (*Wadhams, 1991*). Pancake ice forms through a combination of thermodynamic growth and mechanical thickening, caused by rafting of floes driven by wave motion. This complex growth process is much faster than pure thermodynamic growth and hence may be the main factor responsible for ice edge advance in marginal ice zones. In this paper we present a three-dimensional computer model of pancake ice in a plane wave field. The model uses circular disk-shaped floes in a newly developed discrete element technique (*Hopkins and Tuhkuri, 1999*). The floes are subject to water drag, added mass, gravity, and buoyancy forces. Buoyancy forces for each floe are calculated at each time step from a surface integral. We place a vertical barrier at the end of the simulation domain to represent land fast ice without wave reflection. A drift velocity imparted to the floes by the waves causes the floes to accumulate at the barrier. We calculate the force on the barrier as a function of time and wave amplitude.

## DESCRIPTION OF THE COMPUTER MODEL

The computer model of pancake ice/wave interaction is based on a new three-dimensional discrete element model. A discrete element model is a computer program that explicitly simulates the dynamics of a system of discrete particles. Here the particles are the individual ice floes. The position, orientation, velocity, and shape of each floe are stored in arrays. At each time step, the contact and body forces on each floe are calculated and the floes are moved to new locations with new velocities that depend on the resultant of the forces. The summary presented here is from *Hopkins and Tuhkuri (1999)*.

The ice floes in the simulations are flat disks with a circular edge as shown in Figure 1. The floes are formed by dilating a flat disk of radius  $R_1$  by a sphere with radius  $R_2$ . In the dilation process in mathematical morphology (*Serra, 1986*) the two-dimensional circular disk is transformed into a three-dimensional disk with thickness  $h = 2R_2$  and diameter  $d = 2(R_1 + R_2)$  by placing a sphere with radius  $R_2$  at every point on the two-dimensional circular disk. The aspect ratio of the floe  $d/h$  can be varied by changing  $R_1$  and  $R_2$ . The top and bottom surfaces of the floes are flat.

---

<sup>1</sup>CRREL, 72 Lyme Rd., Hanover, NH 03755 (hopkins@crrel.usace.army.mil)

<sup>2</sup>Clarkson University, Potsdam, NY 13699 (hhshen@clarkson.edu)

Wherever two floes touch, the overlap is interpreted as a deformation of the floes resulting in a contact force. The contact force has components normal and tangential to the surfaces at the point of contact. The normal axis  $\vec{n}$  is perpendicular to the surface of each floe. The tangential axis  $\vec{t}$  is in the direction of the tangential component of the relative velocity at the point of contact. The normal component of the contact force is



Figure 1. Contact between two floes, characteristic of floe rafting (Hopkins and Tuhkuri, 1999).

$$F_n^n = k_{ne} \delta - k_{nv} \vec{V}_{1/2} \cdot \vec{n} \quad (1)$$

The subscript  $n$  denotes the normal direction, the superscript  $n$  denotes the current time step,  $k_{ne}$  is the normal contact stiffness,  $\delta$  is the depth of overlap between the floes,  $k_{nv}$  is the normal contact viscosity, equivalent to a coefficient of restitution, and  $\vec{V}_{1/2}$  is the relative velocity of floe 1 with respect to floe 2 at the point of contact. A value of  $k_{nv}$  near critical damping is used to produce highly inelastic behavior. Tensile forces are not modeled. The incremental change in the tangential force due to friction is proportional to the relative tangential velocity. The tangential force at time  $n$  is

$$\vec{F}_t^n = \vec{F}_t^{n-1} - k_{te} \Delta t (\vec{V}_{1/2} \cdot \vec{t}) \vec{t} \quad (2)$$

where  $\Delta t$  is the time step and  $k_{te}$  is the tangential contact stiffness that is set to 60% of  $k_{ne}$ . The magnitude of  $k_{te}$  affects the rate at which the frictional force increases to the Coulomb limit  $\mu F_n$ , where  $\mu$  is the friction coefficient. If the tangential force  $F_t$  exceeds the Coulomb limit, the  $x$ ,  $y$ , and  $z$  components of  $F_t$  are scaled such that  $|F_t| = \mu F_n$ . The torques on each floe are calculated from the forces and moment arms. The water drag force  $F_d$  on a floe is given by

$$\vec{F}_d = -\frac{1}{2} C_d \rho_w A (\vec{V} - \vec{V}_w) |\vec{V} - \vec{V}_w| \quad (3)$$

where  $C_d$  is the drag coefficient,  $\vec{V}_w$  is the water velocity,  $\rho_w$  is the water density, and  $A = \pi(R_1 + R_2)^2$  is the floe area. The drag force is separated into components normal and tangential to the flat surface of a floe. The drag coefficient  $C_d$ , used in the simulations, was 0.6 for flow normal to the flat surface and 0.06 for flow tangential to the flat surface. The  $x$  and  $z$  components of the water velocity  $U_w$  and  $V_w$  at the floe position  $x$  are

$$U_w = \frac{1}{2} \omega H \cos(kx - \omega t) \quad \text{and} \quad V_w = \frac{1}{2} H \omega \sin(kx - \omega t) \quad (4a,b)$$

where  $H$  is the wave height,  $k = 2\pi / L$  is the wavenumber, and  $\omega = \sqrt{gk}$ . Rotational drag  $M_d$  on a floe is given by

$$M_d = -\frac{1}{2} C_d R_1^2 \rho_w A \vec{\omega} |\vec{\omega}| \quad (5)$$

The three components of the rotational drag are calculated in the body coordinate frame of the floe. The rotational drag coefficient  $C_d$ , used in the simulations, was 0.6 for rotation about the  $x$  and  $y$  body axes (in the plane of the floe) and 0.06 for rotation about the  $z$  body axis (normal to the floe). Water drag was applied only to the underwater floes that were in an exposed position. No drag was applied to floes in the interior of a mass of floes. Added mass was included by multiplying the floe mass by  $I+C_m$  in the equations of motion. The value of the added mass coefficient used in the simulations was 0.15. Hydrodynamic lift was not modeled.

The buoyant force and its moment on each floe was calculated by evaluating a numerical surface integral of the hydrostatic pressure on the floe. The hydrostatic pressure on a differential area element  $d\vec{P}$  was given by

$$d\vec{P} = -\rho_w g(\eta - z)\vec{n}dA \quad (6),$$

where  $\vec{n}$  is the outward normal to the differential element of area  $dA$ ,  $\eta$  is the water surface elevation, and  $z$  is the elevation of the differential element. The equation for the water surface is

$$\eta = \frac{1}{2}H \cos(kx - \omega t) \quad (7).$$

Because it is impractical to calculate the surface integral for each floe at each time step, a look-up table was created. The components of the buoyancy force and moment were calculated for discrete values of 4 independent variables; the depth of the floe center below the actual water surface, the angle between the body  $z$  axis (floe normal) and the global  $z$  axis, the azimuthal angle formed by the projection of the the body  $z$  axis on the global  $xy$  plane and the global  $x$  axis, and finally the inclination angle of the wave surface. A quadri-variate interpolation scheme was used to interpolate between discrete functional values.

After the sum of the forces and torques exerted on each floe have been calculated, the equations of motion for each floe are solved and time advanced. The translational equations of motion use simple central difference approximations. Changes in the angular velocities and orientation of the floes are much more complicated to calculate. We use a method developed by *Walton and Braun* (1993). Euler's equations of motion for the time derivatives of the angular velocities in the principal body frame are solved using a predictor-corrector algorithm. Floe orientations are specified by quaternions. The updated quaternions are found by solving central-difference equations for the time derivatives of the quaternions, expressed in terms of the quaternions themselves and the angular velocities.

In each simulation the change in the kinetic and potential energy of the floes, the energy dissipated by inelastic and frictional contacts and water drag, and the work done by the buoyant force are calculated at each time step. Inelastic and frictional dissipation are determined by computing the work performed by the normal and tangential components of each contact force. The energy balance is used to gauge numerical accuracy. In the simulations described below, the error in the energy balance was less than 2%.

## RESULTS OF THE SIMULATIONS

A set of simulations was performed with the computer model to determine the rate of thickening of the ice accumulation in front of a vertical barrier placed at the end of the model domain. Each simulation began with a single layer of floes distributed uniformly over the water surface with an areal concentration of 50%. The waves moved in the longitudinal or  $x$ -direction toward the barrier. The lateral boundaries of the domain ( $y$ -direction) were periodic. The  $z$ -axis was vertical. The parameters used in the simulations are listed in Table 1.

Table 1. Parameters Used in the Simulations.

Parameter	Symbol	Value
Wave length	$L$	100 m
Wave height	$H$	3,3.5,4,4.5,5 m
Domain length		600 m
Domain width		8.75 m
Floe thickness	$h$	167 mm
Floe diameter	$d$	1 m
Ice density	$\rho_i$	900 kg m <sup>-3</sup>
Water density	$\rho_w$	1010 kg m <sup>-3</sup>
Normal contact stiffness	$k_n$	167 kN m <sup>-1</sup>
Coefficient of restitution	$\varepsilon$	0.25
Floe surface friction	$\mu$	0.35

The non-reflecting barrier, placed at the end of the domain, was intended to simulate land fast ice. The net drift of the floes created an accumulation in front of the barrier. As the accumulation grew, additional floes were added at the other end of the domain at a concentration of 50%. Figure 2a-d shows 4 successive snapshots of the ice accumulation in front of the barrier at 2 second intervals. The wave period  $\sqrt{2\pi L / g}$  was 8 s. The thinning and thickening of the ice accumulation shown in the 4 snapshots shows the alternate longitudinal compression and dilatation produced by the passage of each wave. The series of snapshots in Figure 2 also shows the floe accumulation colliding with the barrier. As the floe accumulation thickens, the force on the barrier increases. The evolution of the force as a function of wave amplitude and time is shown in Figure 3. The rate of increase of the force as a function of wave amplitude is highly non-linear. The results for the case of  $H=3$  m showed nearly zero force and no thickening. We expect the force on the barrier and the ice thickness to reach equilibrium together. In an attempt to reach an equilibrium state of constant force and thickness in the simulation, we concentrated on the  $H=3.5$  m case in the hopes that it would have the smallest equilibrium thickness and thus require the least number of ice floes and the shortest computational time. As shown in the figure the force for  $H=3.5$  m does indeed seem to have reached a sort of plateau, if not equilibrium, after a long period of steady increase.

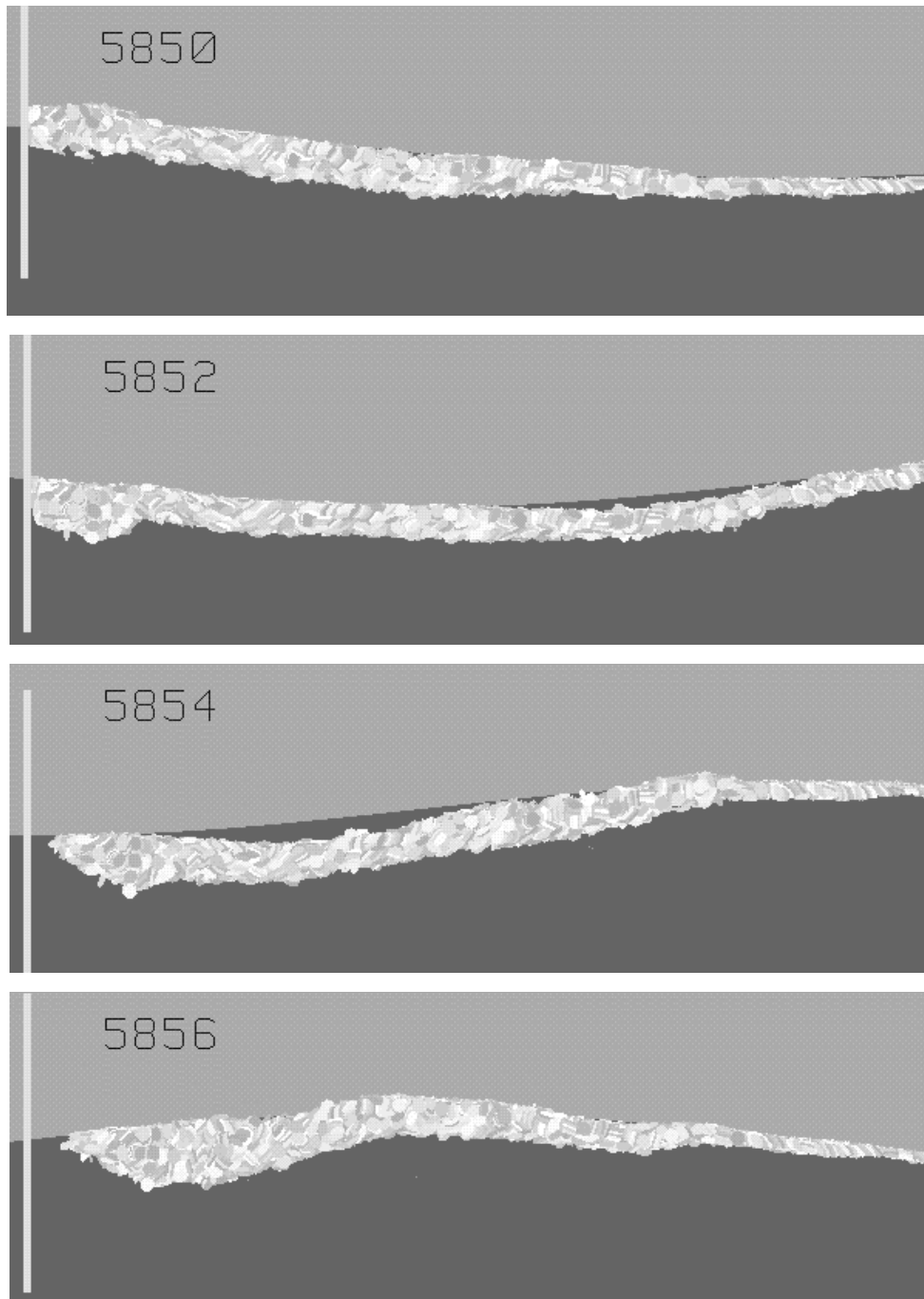


Figure 2a-d. Successive snapshots of the ice accumulation in front of the barrier:  $H=3.5$  m. The width of each figure is 62 m.

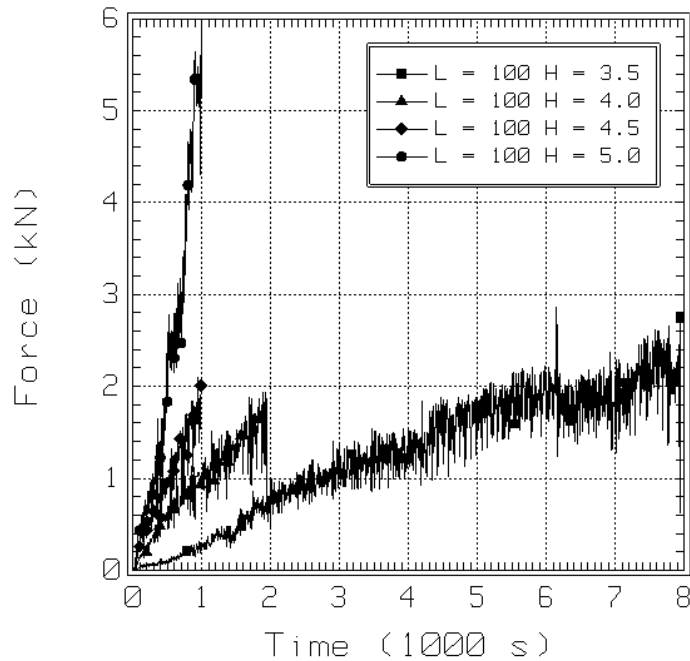


Figure 3. Evolution of the force on the barrier as a function of wave amplitude and time.

## DISCUSSION

From the results of this study, we believe that this computer model is capable of simulating the rafting process central to the formation of pancake ice. Due to its three-dimensional nature and the realistic modeling of water-ice interaction and ice-ice interaction, it closely resembles the physical counterpart. We will use this simulation to determine the functional relation between the rafting thickness and the following parameters: wave amplitude, wavelength, floe diameter, floe thickness, and floe-floe friction. The thickness of the accumulation of rafted ice floe in front of the barrier is a function of the distance from the barrier. It appears that this thickness and the force exerted by the ice against the barrier approach a steady-state value.

## REFERENCES

- Hopkins, M.A., and J. Tuhkuri (1999). Compression of floating ice fields, *J. Geophysical Research*, 104, (C7), 15815-15825.
- Serra, J., Introduction to Mathematical Morphology, *Computer Vision, Graphics, and Image Processing* 35, 283-305, 1986.
- Wadhams, P. (1991) from Notes of IAPSO Workshop on Wave-Ice Interaction, Cambridge Dec. 16-18, 1991.
- Walton, O.R. and R.L. Braun, Simulation of rotary-drum and repose tests for frictional spheres and rigid sphere clusters, *Joint DOE/NSF Workshop On FLOW OF PARTICULATES AND FLUIDS*, Sept. 29 - Oct. 1, 1993, Ithaca, NY.